

Synthesis and Characterization of Heterogeneous Nano-Catalyst for the Production of Biodiesel from Pongamia Pinnata Oil

Aravindh N^{1,*}, Raja S¹, Rajasimman M¹, Vijayakumar.B²

¹Department of Chemical engineering, Annamalai University, Tamilnadu 608002, India

²Department of Petrochemical engineering, RVS College of Engineering and Technology, Tamilnadu 641106, India

Received 26 September 2024; Received in revised form 10 July 2025

Accepted 24 July 2025; Available online 17 December 2025

ABSTRACT

An alternate energy source for a variety of applications is provided by the production of biodiesel from Pongamia pinnata oil. To load MgO onto the ferrite-coated zirconium oxide, the impregnation method was used. A 0.5 mol solution of magnesium nitrate was allowed to dissolve in distilled water. After adding sodium hydroxide and CTAB, the mixture was added to a solution comprising ferrite-coated zirconium oxide and swirled constantly for eight hours at 65°C using a hot plate magnetic stirring device. Once the color of the final solution changed, the introduction of sodium hydroxide was halted. The dense, viscous filtrate was cleaned using methanol and distilled water. After that, the thick sediment was dried by being kept at 110°C for 12 hours in an oven. Lastly, the precursor material was calcined for three hours at 600°C in a muffle furnace. To investigate its catalytic activity, the produced catalyst was evaluated using FTIR, SEM, XRD, and particle size analysis. A maximum yield of 97 wt% biodiesel was attained, when it was transesterified utilizing the ZrO₂/MgO-Fe₃O₄ catalyst under different conditions: 6% (w/w) catalyst concentration, 15:1 methanol to oil molar ratio, 60°C reaction temperature, and 240 min reaction duration. The ASTM standard was utilized for the analysis of the fuel qualities. It appears that the synthesized nanocatalyst is quite responsive in terms of both quality and effectiveness.

Keywords: Doping; Impregnation; Nano catalyst; Pongamia pinnata oil; Transesterification

1. Introduction

Petroleum fuel is used extensively in all facets of our lives. Because the energy sector relies heavily on fossil fuels, their depletion is accelerating over time on a global scale. Additionally, a number of environmental problems have been brought about by the ongoing usage of fossil fuels, which has increased global warming and produced additional pollutants like sulfur oxide and carbon dioxide. Several studies have concentrated on looking for an alternate source in an effort to both meet the world's ever-increasing energy demand and protect the environment. A sustainable and renewable natural source should be used to replace the non-renewable fuel. In comparison to other sustainable sources, biodiesel is now the most appropriate substitute because it is a green fuel with significant potential in place of petroleum diesel. Biodiesel is a fuel derived from renewable sources that is non-toxic, biodegradable, renewable, and environmentally beneficial. It mostly contains free fatty acids and triglycerides.

In the transesterification or esterification process, a short chain alcohol and a catalyst (acidic or base) are employed to convert the presence of free fatty acid and triglycerides to methyl ester. These chemicals are concentrated in vegetable oil and animal fat. Nowadays, edible oils including sunflower, palm, rapeseed, and soybean are the main source of energy for commercial biodiesel, which has a significant impact on the food business. It is always crucial to concentrate on using an inexpensive feedstock since this will cut the price of biodiesel. Non-edible oils are the most viable feedstock as the food industry won't be impacted in any way by their existence. The use of homogenous basic and acid catalysts, such as NaOH, KOH, sulfuric acid, and hydrochloric acid,

has been widespread in many companies. However, due to the emergence of serious issues like environmental pollution, corrosion, and limitations on its selectivity for producing better products, its use in industrial applications has drastically decreased. Because of the strict environmental regulations, there is now a more direct route for the creation of innovative catalysts. According to reports, zeolite and metal oxides are two common solid catalysts utilized in the production of biodiesel. More stable heterogeneous catalysts, such as WO_3/ZrO_2 , $\text{TiO}_2/\text{SO}_4^{2-}$, $\text{ZrO}_2/\text{SO}_4^{2-}$, CaO/ZrO_2 , $\text{Cs-Na}_2\text{ZrO}_3$, $\text{Fe}_3\text{O}_4/\text{KBr}$, and $\text{MgO}/\text{MgAl}_2\text{O}_3$, KF/CaO , Zn/CaO , $\text{KF}/\text{CaO}/\text{Fe}_3\text{O}_4$, and $\text{Cs}/\text{Al}_2\text{O}_3/\text{Fe}_3\text{O}_4$, are found in this acidic or basic heterogeneous catalyst. The existence of water and free fatty acid during the reaction doesn't really affect these catalysts. However, to carry out the reaction at a higher temperature and give it more time has an impact on particular applications. Alkaline earth metal oxides, are supposed to have a larger surface area for improved catalytic activity, which results in selectivity and a longer reaction, both of which improve biodiesel synthesis. When compared to homogenous catalysts, this kind of catalyst has the capacity to be separated more readily from the finished biodiesel product with a higher grade.

Conversely, a solid heterogeneous catalyst with magnetic properties facilitates simple separation from the product through the application of an outside magnetic field. Typically, the spinal type ferrite is used to characterize magnetic catalysts. The characteristics that will stand out the most with the inclusion of ferrite are the increased area and the uniform distribution of the active phase of the particles put onto the surface. There is resistance to both chemical and

thermal affinity in this magnetic nanocatalyst spinel. According to Feyzi and Norouzi [1] the ferrite compounds found in the heterogeneous catalysts exhibit low toxicity, high magnetic property and biocompatibility.

The biodiesel manufacture using zinc-doped magnesium oxide as a nanocatalyst yielded 84.91% [2]. Excellent characteristics of these nanoparticles include activity, selectivity, and recoverability in the biodiesel synthesis process.

Therefore, a nano - catalyst was synthesized in my current study to produce biodiesel from non-edible oil. The synthesized nano-catalyst was examined using various analytical tools such as FTIR, PSA, XRD and SEM. The activity of the nano-catalyst was assessed through transesterification process. The effect of process variables such as methanol to oil molar ratio, catalyst loading (wt %), reaction temperature (K), reaction time (min) were investigated for optimization studies. Finally, the properties of the produced biodiesel were analyzed and compared with the ASTM standards.

2. Materials and Methods

The feedstock, non-edible oil (*Pongamia pinnata*) was procured from “The Arshan Green Organics”, which is a organic product store located in Kotturpuram, Chennai. The chemicals such zirconium oxy chloride hydrate, magnesium nitrate, ferric chloride, ferric sulphate, CTAB, and methanol which are utilized for the synthesising of nano-catalyst and for transesterification reaction were purchased from Merck in India, of analytical grade.



Fig. 1. Preparation of nanocatalyst Fe_3O_4 .

3. Catalyst Preparation

3.1 Preparation of nanocatalyst Fe_3O_4

In a 100 mL SMF flask, 0.5 mol of ferric chloride, 0.25 mol of ferric sulphate, and 0.2 mol of ferric sulphate were added. Deionized water was then allowed to dissolve the mixture. The two samples were combined in a 1000 ml beaker and continuously mixed for one hour at 65°C using a hot plate magnetic stirrer. To create a thick precipitate, 3g of CTAB was added during the reaction. A burette containing 0.1 N of sodium hydroxide was attached to the hot plate magnetic stirrer, and drops of the solution were applied until the color changed and the pH level remained at 11. After being matured for an entire night, the thick, black, solid magnetic precipitate was cleaned three times using methanol and distillate water. The precipitate was calcined, and maintained at 600°C for three hours in a muffle furnace and dried for 12 hours at 110°C in a hot air oven. In order to generate the nanocatalyst Fe_3O_4 - ZrO_2 , two milligrams of ferrite combined with deionized water were added to 0.2 milligrams of zirconium oxy chloride hydrate.

The resultant solution is stirred continuously for an hour by placing it over a hot plate magnetic stirrer. To get a thick precipitate, CTAB was added the resultant solution and after that sodium hydroxide was

added in drop wise in order to look after the pH between 10 to 11. Once the thick blackish precipitate was obtained, it was cooled naturally at room temperature; then after it was washed with distilled water and methanol for thrice and the filtrate was kept for drying overnight at 120°C as shown in Fig. 1.

3.2 Preparation of nanocatalyst MgO/Fe₃O₄-ZrO₂

MgO was loaded onto the ferrite-coated zirconium oxide using the impregnation process. A 0.5 mol solution of magnesium nitrate was allowed to dissolve in distilled water. After adding sodium hydroxide and CTAB, the mixture was added to a solution containing ferrite-coated zirconium oxide and constantly swirled over a hot plate using a magnetic stirring device for eight hours at 65°C. Once the color of the final solution changed, the addition of NaOH was halted. The dense, viscous filtrate was cleaned using methanol and distilled water. After that, the thick precipitate was dried by being kept at 110°C for 12 hrs. in an oven. Lastly, the precursor was calcined for 3 hours at 600°C in a muffle furnace.

3.3 Preparation of biodiesel

The production of biodiesel was carried out in a 500 mL three neck round bottom flask fitted with reflux condenser. After that it was placed over a hot plate magnetic stirrer. Initially oil was added to the round bottom flask and was allowed to heat with continuous stirring to remove the moisture content. Then the mixture of catalyst and methanol was added slowly to one of the necks to study the different parameters affecting the transesterification reaction, such as methanol to oil molar ratio, catalyst loading, reaction temper-

ature and reaction time. After the completion of the reaction, the mixture was allowed to cool and was poured into a separating funnel. The unreacted methanol present in the biodiesel was recovered by using a rotary vacuum evaporator. After the biodiesel product was separated from glycerol, it was washed with warm water and dried at 110°C. The final product was determined gravimetrically as shown in Eq. (3.1).

$$\begin{aligned} \text{Biodiesel Yield (\%)} \\ = \frac{\text{Weight of biodiesel (g)}}{\text{Weight of oil (g)}} \times 100. \end{aligned} \quad (3.1)$$

3.4 Catalyst characterization

The synthesized catalyst was examined to identify the morphology behaviour of the catalyst through various analytical analyses such XRD, SEM, FTIR, PSA and N2 adsorption – desorption measurements.

The crystalline nature of the catalyst was examined using X'pert Pro model, which is working with radiation sources in the range of 2θ (10° to 80°). The catalyst surface area, pore volume and porosity were measured using NOVA 2200 instrument. It was found that surface area for the nanocatalyst was 206.6 m²/g. pore volume was 0.178 cm³/g and pore diameter was found to be 2.2 Å.

The SEM analysis was carried out to identify the morphology of the catalyst using JSM 6360LA. The FTIR was analysed for getting functional group present over the surface of the catalyst in the wave length between 400 to 4000 cm⁻¹ [15].

4. Results and Discussion

Characterization of ZrO₂/MgO-Fe₃O₄ Nano Catalyst:

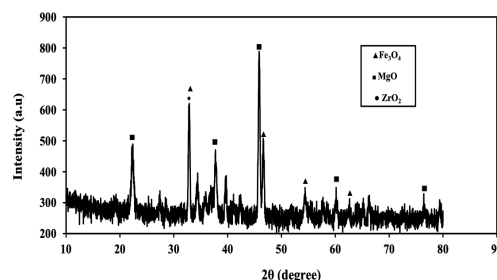


Fig. 2. XRD analysis of $\text{ZrO}_2/\text{MgO-Fe}_3\text{O}_4$ catalyst.

4.1 XRD- analysis

A study was conducted to determine the crystalline nature of the produced nano catalyst ($\text{MgO/Fe}_3\text{O}_4\text{-ZrO}_2$). The development of crystal phases clearly indicates the presence of oxides, which will increase the catalyst's activity and stability. It has been discovered that the $\text{Fe}_3\text{O}_4\text{-ZrO}_2$ surface possesses an amorphous MgO layer, which is represented by a smaller peak at 2θ equal to 37.71° , 45.85° , 60.15 and 76.43 . A strong crystalline phase is indicated by the presence of iron oxide (Fe_3O_4) at 2θ 32.17 , 46.06 , 54.39 , and 62 . Iron oxide and zirconium oxide are strongly attached to each other like cohesive forces because the zirconium oxide presents a tetragonal appearance, notably at the centered position retaining 2θ equal to 37.71 , as illustrated in Fig. 2. Consequently, the crystalline phase may change from tetragonal to monoclinic [6].

4.2 SEM - analysis

According to the SEM analysis of the nanocatalyst ($\text{MgO/Fe}_3\text{O}_4\text{-ZrO}_2$), as illustrated in Fig. 3, the aggregation of magnetic nanoparticles with magnesium results in the formation of condensation plate-like surfaces that induce higher porosity levels. This is because there are more pores, which improve the uniform distribution of particles and allow the particles to take on spher-

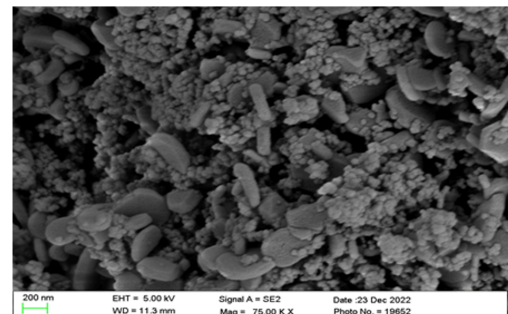


Fig. 3. SEM of $\text{ZrO}_2\text{-CaO-Fe}_3\text{O}_4$ catalyst.

ical shapes.

4.3 FTIR - analysis

The FTIR analysis of the nanocatalyst $\text{MgO/Fe}_3\text{O}_4\text{-ZrO}_2$ core shell during the calcination process is displayed in Fig. 4. The Fe-O particles are evenly distributed across the nano catalyst's surface, giving the appearance of high absorption peaks that induce two phases of vibration: O-Zr vibrations at 622 cm^{-1} and stretching vibrations at 459 cm^{-1} (tetrahedral and octahedral). Strong vibrations of cubic phase nanoparticles are indicated by the presence of MgO , which is detected at 1272 cm^{-1} . The water molecule's existence is demonstrated to be an O-H stretching vibration in the $3400\text{--}3600 \text{ cm}^{-1}$ range [16].

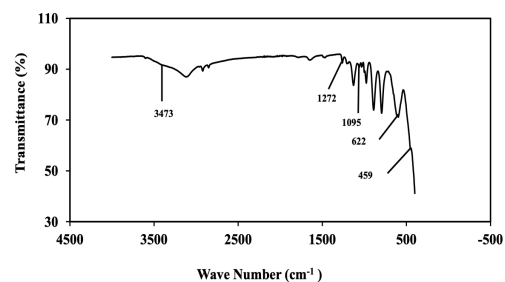


Fig. 4. FTIR spectrum of $\text{ZrO}_2\text{-CaO-Fe}_3\text{O}_4$ catalyst.

4.4 PSA-particle size analysis

The particle size distribution plays a role in determining how much micro dispersion the catalyst can cause in the oil phase of the reaction. The diversity of particle sizes was not very wide, as Fig. 5, demonstrates. This indicates that the catalyst will have little trouble producing a homogeneous distribution in the medium.

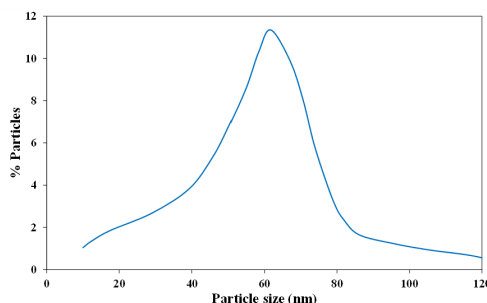


Fig. 5. Particle size analysis.

About 97% of the particles have dispersion between 20 and 100 nm. The desorption technique yielded an overall acid site density of $3473 \mu\text{mol g}^{-1}$ on the catalyst's surface.

5. Transesterification

The parameters optimized to get maximum yield of biodiesel are effect of calcinations temperature, effect of catalyst concentration, effect of methanol to oil ratio, effect of reaction time and effect of reaction temperature [2].

5.1 Effect of methanol to oil molar ratio

The main factor influencing the yield of biodiesel is the alcohol to triglyceride molar ratio. But since transesterification is reversible, extra alcohol is typically added to move the reaction to the product side. The methyl ester concentration rises as the mass ratio of methanol to oil increases because the higher reactant mass ratio in-

creases the contact between the methanol and oil molecules [17].

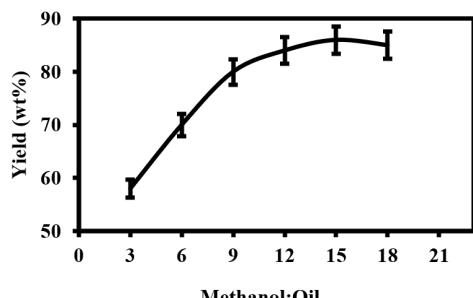


Fig. 6. Effect of the methanol to oil molar ratio.

The catalyst concentration 6%, reaction time 240 minutes, and temperature 60°C were set. The production yield rose along with the rise in the molar ratio of methanol to oil ranging from 3:1 to 18:1. Reduced biodiesel was the outcome of an additional ratio increase. Using $\text{ZrO}_2/\text{MgO-Fe}_3\text{O}_4$ catalysts, the oil to methanol molar ratio was found to be 15:1, yielding the highest yield (86 weight percent) of biodiesel fuel from the *Pongamia pinnata* oil Fig. 6.

5.2 Effect of catalyst concentration

The amount of catalysts employed can have an impact on the production of biodiesel. The transesterification reaction is influenced by the concentration of the catalyst, which works to speed up reaction rates. The effect of varying concentrations was investigated by varying the nanocatalyst concentration within the ranges of 2% to 7% (w/w). As seen in Fig. 7, the highest biodiesel yield of 92 weight percent was achieved with a 6% nanocatalyst concentration. This suggests that the biodiesel yields above 7% are caused by inadequate methanol and oil diffusion; when catalyst concentration rises the biodiesel is absorbed on the catalyst's surface. As the quantity

of heterogeneous catalysts increased, the slurry became excessively viscous, which made mixing difficult and required a lot of power to stir the mixture enough.

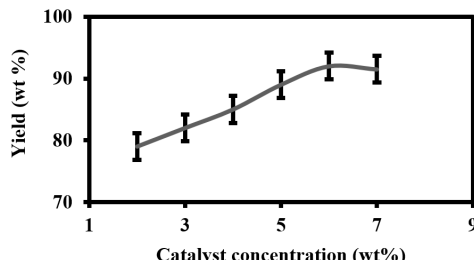


Fig. 7. Effect of the catalyst concentration.

5.3 Effect of reaction time

Methyl ester yield is directly impacted by reaction times. In catalytic activity, the methyl esters increase with increasing reaction time. The conversion of fatty acid esters rises with time, while the prolonged exposure of the catalysts and methanol causes a decrease in yield. Reaction time raises the conversion. Furthermore, as Fig. 8 illustrates, a prolonged reaction time has no effect on the biodiesel production. Under ideal conditions, with a molar ratio of 15:1 methanol to oil and 6% nanocatalyst, the impact of reaction duration on conversion was investigated for varied reaction times ranging from 60 to 360 minutes. When the reaction period was extended to 240 minutes, the biodiesel output rose to 95 weight percent.

5.4 Effect of the reaction temperature

The temperature of the reaction is another significant element that influences the output of biodiesel. The remaining parameters were kept at 6% catalyst and a 15:1 methanol to oil molar ratio for 240 minutes. The temperature range of the reaction was 300–350°K. In addition to increasing the production of biodiesel, a rise in tem-

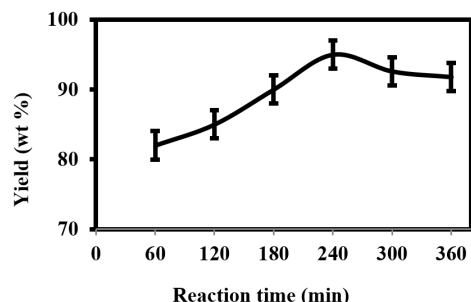


Fig. 8. Effect of the reaction time.

perature also makes a solvent more soluble with a faster diffusion rate. In order to prevent alcohol vaporization leakage, the reaction temperature needs to be lower than the alcohol's boiling point. The oil's viscosity can be reduced by a greater reaction temperature, which will accelerate the reaction and minimize its duration. The outcome shows that at lower temperatures, the conversion of biodiesel was low and grew steadily, reaching 97 & 6 wt% at 333 K. Methanol vaporization is the cause of the output decline, indicating insufficient methanol availability as shown in Fig. 9. The polarity of the methanol, which decreases at higher temperatures, is another factor contributing to the yield decline as temperature rises.

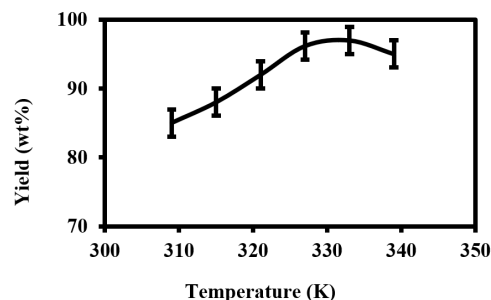


Fig. 9. Effect of reaction temperature.

5.5 Optimized parameters for biodiesel production

Catalyst concentration: 6wt%, methanol to oil molar ratio: 15: 1, reaction time: 240 min and reaction temperature: 333 K to give a maximum biodiesel yield of 97%.

6. Characterization of Biodiesel

Fig. 10, shows the H1NMR range of biodiesel produced under optimum conditions. The singlet signal, which is absent from the oil spectrum and signals the methoxy protons of the ester functionality, at 3.661 ppm verifies the conversion of triglycerides to biodiesel. The biodiesel conversion efficiency was 97%, and its optimum yield of 96.2 wt%. This result indicates that the reaction parameter control has a greater influence on conversion than biodiesel yield [18].

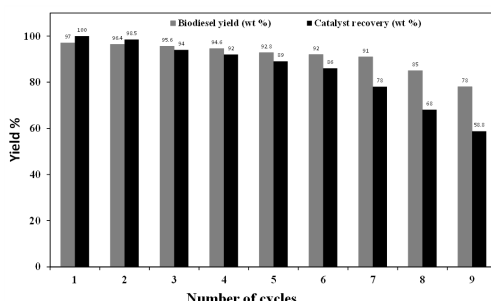


Fig. 10. Reusability of catalyst.

6.1 Reusability of catalyst

The catalyst reusability was studied to reduce the cost of processing the reaction. As the reaction is carried under optimization condition for nine consecutive runs. The catalyst was removed from the reaction mixture by using an external permanent magnet. Then the recovered catalyst was washed with petroleum hexane and methanol to remove the presence of unreacted triglycerides over the surface of the catalyst. It was noticed that up to seven cycles there was not much reduction in yield, but after the seventh cycle yield of biodiesel decreased as shown in Fig. 11 because of the leaching of iron content from the surface of the catalyst. This will lower the active site of the catalyst and, in turn, reduce the conversion of oil to biodiesel [17].

acted triglycerides over the surface of the catalyst. It was noticed that up to seven cycles there was not much reduction in yield, but after the seventh cycle yield of biodiesel decreased as shown in Fig. 11 because of the leaching of iron content from the surface of the catalyst. This will lower the active site of the catalyst and, in turn, reduce the conversion of oil to biodiesel [17].

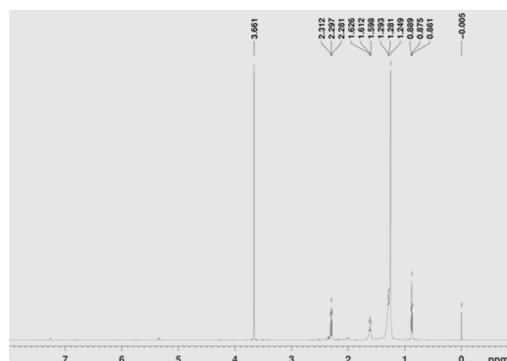


Fig. 11. H^1NMR Spectrum for Biodiesel.

6.2 Fuel properties of biodiesel

The physical – chemical properties of produced biodiesel are shown in Table 1.

Table 1. Physical and chemical properties of produced biodiesel.

Property	Units	Test method	ASTM D6751	Biodiesel
Acid number	mg KOH g ⁻¹	ASTM D664	max 0.5	0.36
Viscosity @40°C	mm ² s ⁻¹	ASTM D445	1.9-6.0	4.2
Flash point	°C	ASTM D93	min 130	142
Cloud point	°C	ASTM D2500	report	18
Water & sediments	vol.%	ASTM D2709	max 0.05	0.05
Sulfated ash	mass %	ASTM D874	max 0.02	0.001
Cetane number	ASTM D613	min 47	60	
Oxidation stability	h	EN 14112	min 3	6.5
Carbon residue	mass %	ASTM D4530	max 0.05	0.032
Phosphorus content	mass %	ASTM D4951	max 0.001	0.0001
Ca & Mg	ppm	EN 14538	max 5	1.8

The properties of biodiesel were compared with ASTM D6751 and were reported. The values of viscosity were found to be low in compression with the given value and found that biodiesel produced from *Pongamia pinnata* oil showed better lubricating characteristics.

7. Conclusion

The biodiesel production from *Pongamia pinnata* oil has demonstrated the efficient catalytic activity of the $ZrO_2/MgO-Fe_3O_4$ heterogeneous nanocatalyst. The nanocatalyst that was created was spherical in shape. $ZrO_2/MgO-Fe_3O_4$ nanoparticles that were calcined at 600°C demonstrated the highest level of catalytic activity. The catalyst concentration is 6 weight percent, the reaction temperature is 333 K, the reaction time is 240 minutes, and the methanol to oil molar ratio is 15:1. These optimized process parameters allow for a maximum biodiesel output of 97%. According to ASTM D6751, the fuel characteristics of *Pongamia pinnata* biodiesel were ascertained. Thus, it can be said that the large-scale generation of biodiesel is appropriate for both *Pongamia* oil and $ZrO_2/MgO-Fe_3O_4$ nanocatalyst.

References

[1] Feyzi M, Norouzi L. Preparation and kinetic study of magnetic $Ca/Fe_3O_4@SiO_2$ nanocatalysts for biodiesel production. *Renewable Energy*. 2016;94:579–586.

[2] Naveenkumar R, Baskar G. Process optimization, green chemistry balance and technoeconomic analysis of biodiesel production from castor oil using heterogeneous nanocatalyst. *Bioresource Technology*. 2021;320:124347.

[3] Aleman Ramirez JL, Reyes Vallejo O, Sanchez Albores R. Development of a reusable CaO/Fe_3O_4 heterogeneous catalyst for biodiesel production.

[4] Wei Y, Han B, Hu X, Lin Y, Wang X, Deng X. Synthesis of Fe_3O_4 nanoparticles and their magnetic properties. 2011.

[5] Hu S, Guan Y, Wang Y, Han H. Nanomagnetic catalyst $KF/CaO-Fe_3O_4$ for biodiesel production. 2011.

[6] Tang S, Wang L, Zhang YS, Wang ST, Wang B. Study on preparation of $Ca/Al/Fe_3O_4$ magnetic composite solid catalyst and its application in biodiesel transesterification. *Fuel Processing Technology*. 2012;95:84–89.

[7] Rezaei R, Mohadesi M, Moradi GR. Optimization of biodiesel production using waste mussel shell catalyst. 2013.

[8] Lal S, Tomer R, Pant D, Thakur RS. Development of $MgSO_4^{2-}/ZrO_2$ heterogeneous catalyst forming biodiesel from Karanja oil.

[9] Uddin MR, Ferdous K, Mondal SK. Preparation of biodiesel from Karanja (*Pongamia pinnata*) oil.

[10] Rao PV, Ramesh S. Optimization of biodiesel parameters (*Pongamia pinnata* oil) by transesterification process.

[11] Khalil MI. Co-precipitation in aqueous solution synthesis of magnetite nanoparticles using iron (III) salts as precursors. 2015.

[12] Suwannasingha N, Kantavong A, Tunkij-janukij S, Aenglong C, Liu HB, Klaypradit W. Effect of calcination temperature on structure and characteristics of calcium oxide powder derived from marine shell waste. 2022.

[13] Buasri A, Chaiyut N, Loryuenyong V, Worawanitchaphong P, Trongyong S. Calcium oxide derived from waste shells of mussel, cockle, and scallop as the heterogeneous catalyst for biodiesel production. 2013.

- [14] Jafari Eskandari M, Hasanzadeh I. Size-controlled synthesis of Fe_3O_4 magnetic nanoparticles via an alternating magnetic field and ultrasonic-assisted chemical co-precipitation. 2021.
- [15] Booramurthy VK, Kasimani R, Subramanian D, Pandian S. Production of biodiesel from tannery waste using a stable and recyclable nano-catalyst: an optimization and kinetic study. *Fuel*. 2020.
- [16] Booramurthy VK, Kasimani R, Pandian S. Nano-sulfated zirconia catalyzed biodiesel production from tannery waste sheep fat. *Environmental Science and Pollution Research*. 2020.
- [17] Balasubramanian R, Sicar A, Sivakumar P, Ashokkumar V. Conversion of bio-solids (sum) from tannery effluent treatment plant into biodiesel. *Energy Sources, Part A: Recovery, Utilization, and Environmental Effects*. 2018.
- [18] Balasubramanian R, Sicar A, Sivakumar P, Anbarasu K. Production of biodiesel from dairy wastewater sludge: a laboratory and pilot scale study. *Egyptian Journal of Petroleum*. 2018.